

# Minigaps and high-density activated transport in $n$ -channel Si inversion layers

J. B. Veiga Salles, H. Closs, and J. R. Senna

*Instituto de Pesquisas Espaciais, 12201 São José dos Campos, São Paulo, Brazil*

P. J. Stiles

*Physics Department, Brown University, Providence, Rhode Island 02912*

(Received 15 September 1987)

We have observed minigap effects on the conductivity of a two-dimensional electron gas on Si surfaces tilted from (001) by an angle  $\theta = 19.5^\circ$ . This is an upper limit of  $\theta$  for observation of such effects. Besides structure in the mobility versus electron concentration, the minigap gives rise to thermal activation of conductance at high concentration. The measured minigap magnitude deviates enormously from the trend deduced from small tilt angles.

The two-dimensional electron gas (2D EG) confined close to the Si-SiO<sub>2</sub> interface of MOSFET's built on Si surfaces tilted away from (001) was shown by Cole, Lakhani, and Stiles<sup>1</sup> to display an anomalous structure in the carrier concentration dependence of the conductivity, corresponding to a discontinuity in the two-dimensional  $E(\mathbf{k})$  dispersion relation of the electrons. This discontinuity was later shown by Sham *et al.*<sup>2</sup> to be due to the lifting, by intervalley coupling, of the two-fold degeneracy of the two-dimensional conduction states originating from the valleys of the Si conduction band with highest mass for motion perpendicular to the interface. Consider the interface to be on the  $(x, y)$  plane. Then the lifting of the degeneracy occurs at the points in the reciprocal  $(k_x, k_y)$  plane where the projection of the three-dimensional ellipsoids of constant energy cross. For an interface obtained by rotation by an angle  $\theta$  around the  $[1\bar{1}0]$  crystalline direction (taken as the  $x$  direction), the two-dimensional dispersion relation  $E(\mathbf{k})$  is given by

$$E(\mathbf{k}) = \hbar^2 k_x^2 / (2m_x) + \hbar^2 (k_y^2 + k_0^2) / (2m_y) \pm [E_G^2 + (\hbar^2 k_0 k_y)^2 / m_y^2]^{1/2}, \quad (1)$$

where  $k_0 = 0.15(2\pi/a)\sin\theta$ , with  $a = 5.43$  Å the lattice parameter of Si, and  $\mathbf{k}_0 = (0, k_0)$  is the projection, on the  $(k_x, k_y)$  plane, of the distance in three-dimensional reciprocal space between the valleys of lowest energy and the Brillouin zone (BZ) edge. The effective masses for in-plane motion are given by<sup>3</sup>  $m_x = 0.19m_0$  and  $m_y(0.19\cos^2\theta + 0.916\sin^2\theta)m_0$ , where  $m_0$  is the free-electron mass. The carrier density at which the anomalies occur is given approximately by the density  $N_s^0$  needed to fill up two independent valleys with the dispersion relation  $E(\mathbf{k}) = \hbar^2 k_x^2 / (2m_x) + \hbar^2 k_y^2 / (2m_y)$  up to  $E_0 = \hbar^2 k_0^2 / (2m_y)$ . Then  $N_s^0 = 95.89(m_x /$

$m_y)^{1/2} \sin^2\theta (10^{12} \text{ cm}^{-2})$ . This dependence on  $\theta$  verified experimentally by Sham *et al.*<sup>2</sup> and confirms the validity of the valley-projection model.

For a Si MOSFET, the breakdown field of the order approximately  $10^7$  V/cm, limits  $N_s$  to be  $\lesssim 2 \times 10^{12} \text{ cm}^{-2}$ , and therefore the tilt angles for observation of effects of the minigap on transport are limited to  $\theta \lesssim 19.5^\circ$ . We have measured the structure in conductivity  $\sigma$  and  $d\sigma/dT$  in a set of (114) ( $\theta = 19.5^\circ$ ) samples up to  $N_s = 9.5 \times 10^{12} \text{ cm}^{-2}$  (close to actual breakdown for the samples), and determined the value of  $E_G$ , kept as an adjustable parameter in Eq. (1), by fitting the experimental results with transport calculations.

The conductivity tensor for a 2D EG in the presence of a minigap was first calculated by Ando,<sup>4</sup> with a model zero-range correlation length for the scatterers, neglecting the anisotropy of the effective masses. We choose instead to evaluate it by writing

$$\sigma_{xx}(N_s, T) = \int_0^\infty d\epsilon [-\partial f(\epsilon) / \partial \epsilon] \sigma_{xx}(\epsilon, T), \quad (2)$$

with

$$\sigma_{xx}(\epsilon, T) = \sum_{\mathbf{k}} v_x^2(\mathbf{k}) A(\mathbf{k}, \epsilon) \tau_{xx}[E(\mathbf{k})] / (2\pi), \quad (3)$$

where  $v_x(\mathbf{k})$  is calculated from the dispersion relation Eq. (1), and  $A(\mathbf{k}, \epsilon)$  is the spectral function, given by

$$A(\mathbf{k}, \epsilon) = 2\Gamma(E(\mathbf{k})) \{ [\epsilon - E(\mathbf{k})]^2 + \Gamma^2[E(\mathbf{k})] \}^{-1}. \quad (4)$$

The broadening parameter  $\Gamma$  and the transport relaxation time  $\tau_{xx}$  are calculated in the independent-valley approximation, by a rescaling in momentum space:  $k_x = (m_x / m_y)^{1/2} g_x = (m_x / m_y)^{1/2} g \cos\phi$ ,  $k_y = (m_y / m_x)^{1/2} g_y = (m_y / m_x)^{1/2} g \sin\phi$ . We obtain the results

$$\Gamma(\epsilon) = (4\pi^2)^{-1} \int_0^{2\pi} d\phi \int_0^{2\pi} d\phi' \langle V^2(\mathbf{k} - \mathbf{k}' = \mathbf{q}(\epsilon, \phi, \phi')) \rangle, \quad (5)$$

$$\tau_{xx}^{-1}(\epsilon) = (2\pi^2)^{-1} \int_0^{2\pi} d\phi' \langle V^2(\mathbf{k} - \mathbf{k}' = \mathbf{q}(\epsilon, \phi, \phi')) \rangle \cos\phi(\cos\phi - \cos\phi'), \quad (6)$$

with analogous expressions for  $\sigma_{yy}$ .<sup>5</sup> The last result is the lowest-order in an expansion of the nonequilibrium distribution in  $\cos(n\phi)$  terms. The disorder-averaged square matrix element of the scattering potential is given by a sum of contributions from  $\text{Na}^+$  impurities (characterized by a surface density  $N_{\text{ox}}$ ) and from interface roughness in the Si-SiO<sub>2</sub> interface (characterized by rms fluctuation  $\Delta$  with correlation length  $\Lambda$ ).<sup>6</sup> We have not taken into account the temperature dependence of the screening function.

Standard<sup>7</sup> measurements of  $\sigma_{xx}$  and  $\sigma_{yy}$  at 4.2 K were performed on MOSFET's fabricated on (114) surfaces by Toshiba Co.; such samples are described in a paper by Sato *et al.*<sup>8</sup> The smooth structures in mobilities for

channel current along or perpendicular to the  $[1\bar{1}0]$  axis ( $x$  and  $y$  directions, respectively), due to the presence of a minigap, are better revealed by plotting the derivatives of these mobilities with respect to  $N_s$ , as shown in Figs. 1(a) and 1(b) for the electron concentration range in which the deviation from the behavior with vanishing gap occurs. Minigap sizes are known<sup>9-11</sup> to increase with  $N_s$  as our calculation does not account for an explicit dependence of the gap on surface electron density, we choose to fit the experimental data in the neighborhood of  $N_s = 7.5 \times 10^{12} \text{ cm}^{-2}$ , where both  $d\mu^{-1}/dN_s$  for  $x$  and  $y$  current directions have a sharp peak. The best fit (solid curves in Fig. 1) corresponds to  $E_G = 0.2E_0 = 9.4 \text{ meV}$ . Theoretical curves using other gap values differ from the experimental results regarding the  $N_s$  locus, width, and amplitude of the minigap structures, as shown in Figs. 1(a) and 1(b). The mobility anisotropy ratio  $\mu_{xx}/\mu_{yy}$  undergoes a sharp change in behavior as a function of  $N_s$  as the Fermi level approaches the minigap region, as can be seen in Fig. 1(c). The theoretical curves in Fig. 1 were calculated with  $\Lambda = 15 \text{ \AA}$ ,  $\Delta = 3.9 \text{ \AA}$ , and  $N_{\text{ox}} = 0.28 \times 10^{12} \text{ cm}^{-2}$  for sample 1X, and  $\Lambda = 15 \text{ \AA}$ ,  $\Delta = 4.9 \text{ \AA}$ , and  $N_{\text{ox}} = 0.15 \times 10^{12} \text{ cm}^{-2}$  for sample 2Y.

A further consequence of the  $E(\mathbf{k})$  discontinuities is a sharp effect in the temperature dependence of conductivity, experimentally observed as a structure in the dependence of  $d\sigma_{ii}/dT$  on  $N_s$ , as shown in Fig. 2. The experimental data refer to the same samples, but were obtained at 13 K by directly measuring the amplitude of conductance oscillations due to natural 2.4-Hz temperature oscillations in the cold end of a Displex Closed-Cycle CSA-202 refrigeration system. The dashed curves in that figure show the theoretical results for the same parameters which give the best fit for the 4.2-K mobility derivatives. We have also observed such  $d\sigma/dT$  structures in (118) surfaces in connection with minigap effects,<sup>1</sup> and interpret them as due to the thermal promotion of carriers across the disorder-broadened discontinuities in the energy dispersion relation. In (114) surfaces, for current along the valley-overlap direction  $y$ , such effect gives rise to conductance activation for  $N_s \geq 7.7 \times 10^{12} \text{ cm}^{-2}$ , as shown in Fig. 2. Such interpretation is supported by the

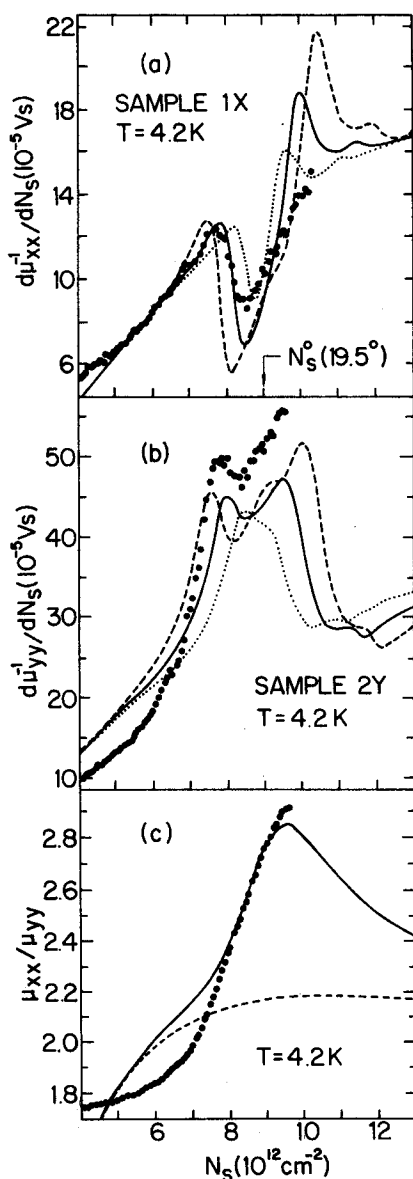


FIG. 1. (a) Measured (circles) and calculated (solid line for  $E_G = 0.2E_0$ ; dashed line for  $E_G = 0.3E_0$ ; dotted line for  $E_G = 0.1E_0$ ) derivatives of inverse mobility with respect to  $N_s$ , for current in the  $x$  direction (parallel to  $[1\bar{1}0]$ ); (b) same as (a) for current in the  $y$  direction (perpendicular to  $[1\bar{1}0]$ ); (c) measured (circles) and calculated (solid line for  $E_G = 0.2E_0$ ; dashed line for  $E_G = 0$ ) mobility anisotropy as a function of  $N_s$ .

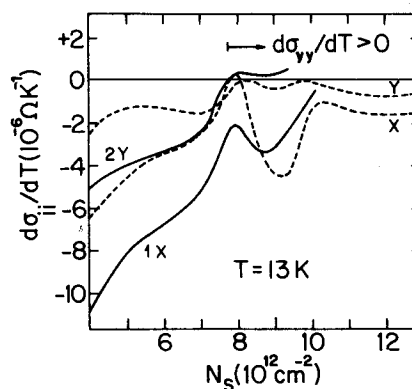


FIG. 2. Directly measured (solid curves) and calculated (dashed curves) temperature derivatives of conductivity as a function of  $N_s$ , for current perpendicular and parallel to  $[1\bar{1}0]$ . The arrow indicates the onset of conductivity thermal activation for channel current in the  $y$  direction.

present calculation, which predicts the form and loci of the  $d\sigma_{ii}/dT$  structures, although their calculated values differ from those measured at 13 K, probably because our calculation does not take the temperature dependence of screening into account.

So far, no theory has succeeded in predicting actual minigap magnitudes.<sup>12</sup> Approximations based on  $\mathbf{k}\cdot\mathbf{p}$  expansions around the  $X$  points<sup>13,14</sup> and  $\Gamma$  point<sup>14</sup> of the Si BZ have been proposed, but the gap sizes they predict are systematically far smaller than the measured ones. Different empirical relations were proposed by Tsui and Gornik,<sup>9</sup> Sesselmann and Kotthaus,<sup>10</sup> and Kamgar, Sturge, and Tsui<sup>11</sup> to fit spectroscopic results for the dependence of gap size on surface electron density, Fermi wave vector, and tilt angle  $\theta$ , up to  $\theta=9^\circ$ . Data for  $10^\circ$  and  $12.3^\circ$  were shown<sup>10</sup> to depart from a  $E_G \propto (A + B \sin^2\theta)N_s$  trend observed for lower  $\theta$ . No experimental results were reported for  $\theta > 12.3^\circ$ , except for Lakhani, Cole, and Stiles,<sup>15</sup> who using circular (115) samples have estimated  $E_G(15.8^\circ) \approx 2.5E_G(10^\circ)$ , which would fit the low-angle behavior. The 9.4-meV gap which simultaneously fits our  $d\mu_{ii}^{-1}/dN_s$ ,  $\mu_{xx}/\mu_{yy}$ , and  $d\sigma_{ii}/dT$  experimental results for  $\theta=19.5^\circ$  at  $N_s=(7.5\pm0.5)\times10^{12}\text{ cm}^{-2}$  deviates enormously from any of the empirical relations cited above, and confirms the departure initiated near  $10^\circ$ . This is shown in Fig. 3, where  $E_G(N_s^0)/N_s^0$  for  $\theta=(19.5\pm0.5)^\circ$  is compared to data reported so far<sup>2,10,11</sup> for  $2.9^\circ \leq \theta \leq 12.3^\circ$ . The vertical bar corresponding to  $19.5^\circ$  was obtained extrapolating  $E_G$  from  $N_s=(7.5\pm0.5)\times10^{12}\text{ cm}^{-2}$  to  $N_s^0(19.5^\circ)=8.9\times10^{12}\text{ cm}^{-2}$  with  $1.1 \leq dE_G/dN_s(10^{-12}\text{ meV cm}^{-2}) \leq 2.2$ , that is, within the limits experimentally observed of  $dE_G/dT$  for other tilt angles. The dashed line in that figure is the theoretical prediction which results approximating the solution to Eq. (1) by a  $\mathbf{k}\cdot\mathbf{p}$  expansion around the  $X$  point,<sup>12-14</sup> the expansion around the  $\Gamma$  point leads to normalized gaps smaller than  $0.3\times10^{-12}\text{ meV cm}^{-2}$  for the  $\theta$  range of Fig. 3.

In conclusion, we have measured for the first time the minigap in an inversion layer tilted from the (001) surface by the highest angle ( $19.5^\circ$ ) allowing observation of such effects. We have observed corresponding anomalies in

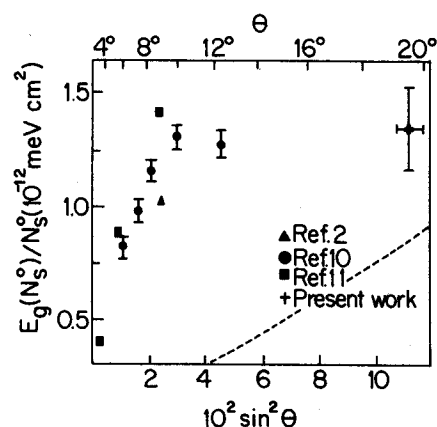


FIG. 3. Present ( $\theta=19.5^\circ$ ) and previously reported normalized gaps  $E_G(N_s^0)/N_s^0$ . Data from Ref. 11 were extrapolated by means of Eq. (3) and Table I of that reference. Another value for  $\theta=10^\circ$  extrapolated from results in Ref. 1 essentially coincides with the above one from Ref. 10. The dashed line is the theoretical prediction based on a  $\mathbf{k}\cdot\mathbf{p}$  expansion around the  $X$  point.

the dependence of mobility on electron density at low temperature, and have directly measured the derivative of conductance with temperature at 13 K. For such a large tilt angle, the anomalies occur in a region of concentration where the mobility is decreasing with concentration and this, coupled with the minigap in the electronic dispersion, gives rise to a novel thermal activation of channel conductivity at high electron densities. These features of conductivity are well explained by the normal theory of transport in inversion layers, when modified to take into account the effect of a minigap caused by valley splitting. The magnitude of the splitting obtained from fitting theory to experiment is found to be far smaller than expected from the behavior observed for low tilt angles.

The authors would like to thank Y. Takeishi and H. Maeda, of the Toshiba Research and Development Center, who generously provided the samples used in this work.

<sup>1</sup>T. Cole, A. A. Lakhani, and P. J. Stiles, Phys. Rev. Lett. **38**, 722 (1977).

<sup>2</sup>L. J. Sham, S. J. Allen, Jr., A. Kamgar, and D. C. Tsui, Phys. Rev. Lett. **40**, 472 (1978).

<sup>3</sup>F. Stern and W. E. Howard, Phys. Rev. **163**, 816 (1967).

<sup>4</sup>T. Ando, J. Phys. Soc. Jpn. **47**, 1595 (1979).

<sup>5</sup>Obtained by replacing  $\cos\theta$  and  $\cos\theta'$  by  $\sin\theta$  and  $\sin\theta'$ , respectively. The screened potentials depend both on the magnitude and direction of  $\mathbf{k}-\mathbf{k}'$ , since the polarizability of an anisotropic 2D EG is also anisotropic.

<sup>6</sup>T. Ando, J. Phys. Soc. Jpn. **43**, 1616 (1977).

<sup>7</sup>F. Fang and A. B. Fowler, Phys. Rev. **169**, 619 (1968).

<sup>8</sup>T. Sato, Y. Takeishi, H. Hara, and Y. Okamoto, Phys. Rev. B **4**, 1950 (1971).

<sup>9</sup>D. C. Tsui and E. Gornik, Appl. Phys. Lett. **32**, 365 (1978).

<sup>10</sup>W. Sesselmann and J. P. Kotthaus, Solid State Commun. **31**, 193 (1979).

<sup>11</sup>A. Kamgar, M. D. Sturge, and D. C. Tsui, Phys. Rev. B **22**, 841 (1980).

<sup>12</sup>A review of the results up to 1979 is given by V. A. Volkov, V. A. Petrov, and V. B. Sandomirskii, Usp. Fiz. Nauk **131**, 423 (1980) [Sov. Phys.—Usp. **23**, 375 (1980)].

<sup>13</sup>F. J. Ohkawa, J. Phys. Soc. Jpn. **45**, 1427 (1978).

<sup>14</sup>L. J. Sham, in *Physics of Semiconductors, 1978*, edited by B. L. Wilson (Institute of Physics, Bristol, 1979), p. 1339.

<sup>15</sup>A. A. Lakhani, T. Cole, and P. J. Stiles, Surf. Sci. **73**, 223 (1978).